Designing LiDAR-equipped UAV Platform for Structural Inspection

M. Nasrollahi[a] , N. Bolourian[a] , Z. Zhu[a] and A. Hammad[b]

[a]Department of Building, Civil, and Environmental Engineer, Concordia University, Canada
[b]Concordia Institute for Information Systems Engineering (CIISE), Concordia University, Canada
E-mail: m_nasro@encs.concordia.ca, n_bolour@encs.concordia.ca, zhenhua.zhu@concordia.ca, ma

Abstract –

Efficient inspection and maintenance of bridges are vital for improving safety and sustainability of infrastructure systems. Recently, Light Detection and Ranging (LiDAR) scanners are used for detecting surface defects. The LiDAR scanner can be mounted on an Unmanned Aerial Vehicle (UAV), which provides easier accessibility to most parts of the structure and can fly close to the structure. There are two types of mobile LiDAR scanners: 2D and 3D. A 2D scanner is more affordable, but it can only scan points on a plane. However, a 2D scanner can be transferred into 3D scanner by rotating the scanner using a servo motor. This paper aims to design a platform for LiDAR-equipped UAV for structural inspection using an affordable 2D scanner. First, the requirements and other design considerations are introduced. Then, the design details and the hardware and software integration steps of the LiDAR-equipped UAV platform are discussed. The initial test of the platform showed that it can provide acceptable accuracy for detecting large defects.

Keywords –
LiDAR; UAV; Structural Inspection

1 Introduction

Efficient inspection and maintenance of bridges and other structures are vital for improving safety and sustainability of infrastructure systems. Traditionally, visual inspection using non-equipped eyes and manual measurements are used for detecting surface defects, which may lead to subjective results. This approach is time-consuming and unsafe, especially for inspecting the inaccessible elements of a bridge [1].

Recently, 3D Light Detection and Ranging (LiDAR) scanners [2] and cameras [3] are used for detecting surface defects (e.g. cracks) using computer vision methods. In general, LiDAR technology is more expensive than cameras, and defect detection results

may miss some edge points. However, it is a promising method, not only for detecting the location and size of the defects but also for computing their depth and volume [4, 5]. Also, unlike digital images, the generated point clouds are not affected by lighting, and their analysis does not require supplementary information [6].

The LiDAR scanner can be mounted on a tripod [1] (i.e. terrestrial scanning) or on an Unmanned Aerial Vehicle (UAV) [7, 8] (i.e. aerial scanning). Although terrestrial scanning provides high stability for the scanner and less vibration, it is not time efficient. The aerial scanning provides easier accessibility to most parts of the structure and can fly close to the structure. Consequently, higher coverage of the inspected surfaces and more accurate results can be achieved.

In addition, the LiDAR-equipped UAV eliminates the inspectors' falling risks encountered in the traditional inspection method. The risk of damages caused by the UAV is low because of its size, weight, and controllability [10]. The Special Flight Operation Certification (SFOC), required by the Canadian Aviation Regulations, includes the plan of operation respecting specific safety rules, such as the distance between the operators and UAV, keeping people away from the flight site, and flying the UAV in the Line of View (LoV) [11].

LiDAR-equipped UAVs are used in different applications such as surveying [12], inspection [13], navigation [14], and agriculture [15]. There are two types of mobile LiDAR scanners: two dimensional (2D) and three dimensional (3D). A 2D scanner is more affordable, but it can only scan points on a plane, while a 3D scanner can capture the point cloud of the surrounding space, which makes the data more accurate. However, a 2D scanner can be transferred into 3D scanner by rotating the scanner using a servo motor [16] or by moving the scanner on a robot/UAV while collecting the point cloud [17]. The accurate rotational positions of the servo or the Simultaneous Localization And Mapping (SLAM) algorithm can be used to register the collected data. For example, in the research of Winkvist et al. [17] and Bachrach et al. [14], a 2D

LiDAR is mounted on the top of a UAV, and SLAM is used for generating the point cloud taking advantage of the vertical movement of the UAV. In order to increase the Field of View (FoV) of the scanner, in the ARIA project [16] a servo mounted on the UAV is used to rotate the scanner while the UAV is flying, which leads to collecting 3D point clouds for inspection and navigation purposes. However, the details of the platform design for integrating the UAV, the servo and the scanner are not available in the literature.

The objective of this paper is to design a platform for LiDAR-equipped UAV for structural inspection using an affordable 2D scanner. The remaining sections of the paper are as follows: First, the requirements and other design considerations are introduced in Section 2. Section 3 provides the design details and the hardware and software integration steps. Section 4 provides an initial test of the platform. Section 5 provides the conclusion and summary of future work.

2   Design Considerations

In order to have a successful design of the LiDAR-equipped UAV, the following should be considered:

2.1   Objectives

The maximum coverage of the surface of the inspected structure and the minimum cost are the two main objectives of an efficient inspection using the LiDAR-equipped UAV. The main costs of this method are the equipment cost and the flight cost. The flight cost depends on the time of the flight. The full coverage may not be achieved because of the obstacle near the inspected structure, which can limit the visibility of the LiDAR. So, the path planning goal is finding a collision-free path with minimum time-of-flight and maximum coverage.

2.2   Requirements

In order to choose the most appropriate LiDAR-equipped UAV, all the following requirements should be considered with respect to the budget.
(1) Mounting location: Most of the commercially available solutions have the scanner mounted under the UAV because they are designed for surveying purposes (Figure 1(c)). However, for structural inspection purposes, the LiDAR can be mounted either on top (Figure 1(a) and (b)) or under the UAV depending on the location of the inspected area of the structure.
(2) Metrology method: There are two types of metrology methods for LiDAR: Time-of-Flight (ToF) and Phase Shift (PS). ToF is used for long range of measurement with the accuracy of 4-10 mm at 100 m. Unlike ToF, PS is practical for short range of

(a) MIT RANGE [14]   (b) CMU ARIA [29]

(c) Stormbee [28]

Figure 1. Scanner position on top of UAV in (a) and (b), and under UAV in (c)

measurement with 2-4 mm at 20 m [1].
(3) Maximum payload: The maximum payload is the weight that the UAV is capable to carry. Therefore, the weight of all carried devices (e.g. scanner, minicomputer, batteries, and GPS) should not exceed this threshold. The payload affects the UAV time of flight because carrying a heavier payload consumes more energy. As the weight of the scanner is one of the major weights in the payload of the UAV, it should be carefully considered. Providing a light and accurate scanner is expensive, and choosing the best option depends on the available budget. Moreover, extra batteries are needed to supply the power for the scanner and other electronic parts attached to the UAV (e.g. servo, microcomputer, etc.).
(4) Size of UAV: The UAV should be big enough to carry the scanner and other equipment, and small enough to fly safely as close as possible to the inspected surface.

2.3   Constraints

There are several constraints which should be considered during the planning.
(1) Minimum and maximum distances: A specific distance range should be considered during inspection based on safety and the characteristics of the scanner. The density of the scanned point cloud decreases with longer distances.
(2) Battery capacity: The battery capacity has effects on the time of flight. As mentioned above, although adding more batteries helps the UAV to fly further, it increases the weight of the system.
(3) Vibration: The vibration of the LiDAR-equipped

UAV during inspection causes errors. A suitable design of a LiDAR-equipped UAV, which includes designing an appropriate engine and body shape, installing dampers, etc., can decrease the vibration [18].

(4) Degrees of Freedom (DoFs): Each UAV has six DoFs: three displacements (x, y, and z) and three rotations (roll, pitch, and yaw). In general, the pitch and roll of the UAV are constrained to keep the UAV in a horizontal position.

(5) LiDAR parameters: The 2D and 3D scanners have one and two FoVs, respectively. The FoV is an important parameter in the visibility analysis. Furthermore, other important parameters of the scanner are the angular resolution ($\Delta\theta$), incidence angle (θ), and beam diameter (Figure). The accuracy of a point cloud is mainly related to the measurement resolution, angular resolution and scanning speed. In the case of the 2D scanner integrated with a servo, the angular resolution and the speed of the servo affect the accuracy of the generated point cloud.

2.4   Other considerations

(1) Safe operation: Mounting additional devices should not change the center of gravity of the UAV because it effects on the stability of the UAV. Also, the additional devices should not interrupt the GPS signals.

(2) Real time: The LiDAR-equipped UAV platform has to collect a large amount of point cloud data to be used in real time for path planning and obstacle detection.
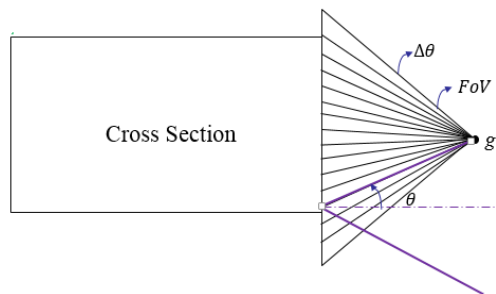
Figure 2. Some specifications of the LiDAR

3   Platform Design

UAV selection

DJI Matrice 100 [19] is used in this platform because it is customizable and has expansion bays to mount the scanner and other devices on top or below the UAV. Also, its radius is less than one meter, which makes it agile and able to enter narrow spaces near the inspection surfaces. The specifications of this UAV are shown in Table 1. The maximum payload is about 1.2 Kg.

Table 1. UAV specifications

Specification	Value
Max takeoff weight	3.60 Kg
Net weight	2.43 Kg
Battery	5700 mAh – 22.8V
Diameter	996 mm
Hovering time (no payload)	28 minutes

LiDAR selection

Hokuyo UTM-30LX 2D laser range finder is used for data collection because of its light weight and affordable price [20]. The specifications of this scanner are shown in Table 2.

Table 2. Scanner specifications [19]

Specification	Value
Detection range	0.1 ~ 30m
Accuracy	±30mm (under 10m)
Horizontal FoV	270º
Angular resolution	0.25º
Scan speed	43,200 points per second
Weight	210 g (without cables)

Servo selection

In order to enable the scanner to generate a 3D point cloud, a servo is used to rotate it. Dynamixel MX-28T is a robotic actuator servo that can control the movement of the scanner with a minimum step of 0.088º, which means the angular resolution of the platform is 0.088º. By rotating the scanner 180º, the vertical FoV of the scanning becomes 360º.

The servo uses an adapter (USB2Dynamixel) to connect to the microcomputer and another adapter (SMPS2Dynamixel) to connect to the battery. Both the servo and the scanner need a 12V power supply.

Microcomputer selection

To control the scanner and the servo, and to collect data from them in real time, DJI MANIFOLD microcomputer is selected in this platform because it is compatible with the UAV [21]. The power for MANIFOLD is supplied directly from the UAV.

Electronic connectors

An isolated voltage regulating board is designed and built to convert the 25V power of UAV's port into 12V. This board makes it possible to run the scanner and servo without adding an extra battery. The weight of the voltage regulating board is 72 g.

Interfacing parts using 3D printing

Although previous research exists about interfacing a servo with 2D LiDAR [22] , the integration with the

UAV requires additional interfaces to control the direction of the scanning. Three different interfacing parts are designed and 3D printed to attach the scanner and the servo to each other and to the UAV. The designed parts are shown in Figure 3. Figures 3 (c) and (d) show the parts for attaching the servo to the UAV in vertical or inclined positions, respectively.

(a) Part for holding servo

(b) Part for holding scanner

(c) Part for attaching servo vertically

(d) Part for attaching servo inclined
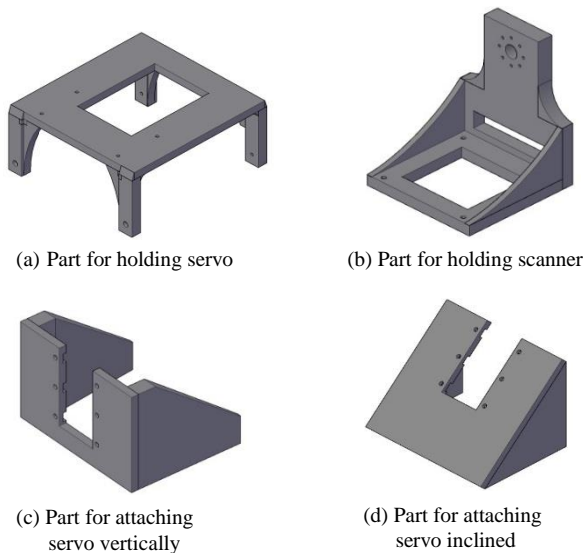
Figure 3. Design of interfacing parts for 3D printing

3.1 Integration

To integrate the components, hardware and software integrations are required. These are discussed in the following sections.

3.1.1 Hardware Integration

Figure 4 shows the integration of the hardware components of the platform. Table 3 shows the summary of hardware specifications and their connectivity to each other. The total weight of the integrated platform is 3.13 Kg, which is less than the maximum takeoff weight of the UAV.

In this platform, the scanner rotates 180º (from -90º to 90º). It stops for 0.1 s when changing direction from clockwise to counterclockwise. This stop causes some errors in the registration process of the point cloud. It is possible to rotate the scanner continuously in one direction by adding a slip-ring between the scanner and the servo to eliminate the rotation of the cables of the scanner. Figure 5 shows the interfacing part for mounting the servo on the UAV vertically or with inclination, and the corresponding configurations of the LiDAR-equipped UAV platform.

3.1.2 Software Integration

Spin Hokuyo Robot Operating System (ROS) software package is installed on the microcomputer to create 3D point clouds in real time [23]. This software works under Ubuntu operating system and contains the code to control the servo and the scanner to generate a 3D point cloud. Spin Hokuyo has five nodes for the following purposes: (1) two nodes (tilt motor and tilt transform) for controlling the servo and assembling point cloud messages; (2) one node (Hokuyo robot filter) to remove unnecessary points that are related to the body of the operating robot. It eliminates all the points inside the radius of 50 centimeters; (3) one node (scan to PCL (Point Cloud Library)) to convert the scanned data into point cloud messages; and (4) one node (PCL assembler client) to combine all the published point cloud messages into one point cloud message. Spin Hokuyo can adjust the initial, start and end positions of the servo and its rotation speed. The SLAM algorithm can be used in the software package to enable the platform to scan during the UAV flight.
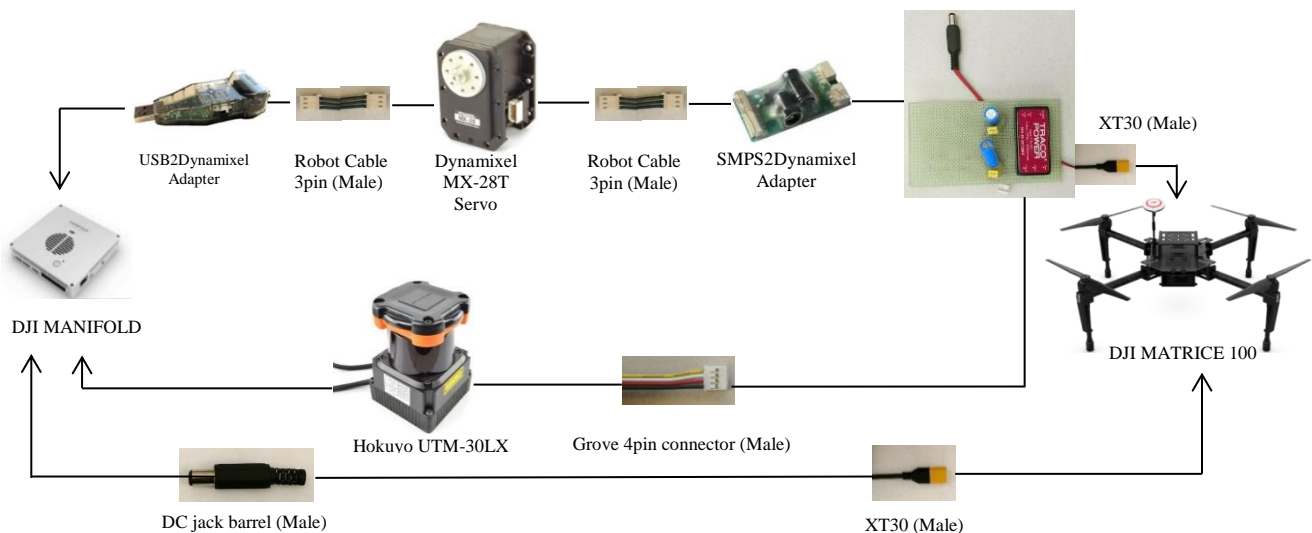
Figure 4. Hardware integration

Table 3. Summary table of hardware components

Component	Function	Voltage (V)	Current (A)	Weight (g)	Attached to
Hokuyo UTM-30LX	Laser Scanning	12	1.0	210	MANIFOLD, Voltage Regulator Board
MANIFOLD	Controlling scanner and Servo	14-26	Up to 10	197	UAV, USB2Dynamixel Adapter, scanner
Dynamixel MX28T	Rotating scanner	12	1.4	72	USB2Dynamixel Adapter, SMPS2Dynamixel Adapter
USB2Dynamixel Adapter	Connect servo to MANIFOLD	N/A	N/A	28	Servo, MANIFOLD
SMPS2Dynamixel Adapter	Power supply for servo	12	1.4	14	Servo, Voltage Regulator Board
Voltage Regulator Board	Regulate the voltage to 12V	9-36	3.3	72	SMPS2Dynamixel Adapter, scanner, UAV
Part for holding servo	Connect servo and scanner to UAV	N/A	N/A	45	UAV, 3D printed servo part
Part for attaching servo vertically	Connect servo to the table part	N/A	N/A	26	Servo, 3D printed table part
Part for attaching servo inclined	Connect servo to the table part	N/A	N/A	29	Servo, 3D printed table part
Part for holding scanner	Connect scanner to servo	N/A	N/A	31	Servo, scanner

After scanning, the point cloud that is generated by Spin Hokuyo can be visualized in Rviz (ROS 3D visualization tool) [24]. Rosbag package records the output messages of spin Hokuyo and save them as Bag file [25]. There is a node named *Bag to PCL* in PCL-ROS package, which reads the Bag file and converts ROS point cloud messages to PCD (Point Cloud Data) files [26] CloudCompare software can open and visualize PCD point cloud files, and convert them to other point cloud file formats, such as LAS, LAZ and E57 [27].

In this work, Spin Hokuyo is used in a stationary mode for initial testing as explained in Section 4. When integrated with In the case of flying on a UAV, because the GPS signals may not be available when the UAV is flying under a bridge., Therefore, other localization methods can be investigated, such as integrating an onboard Inertial Measurement Unit (IMU) with Visual Odometry (VO), Simultaneous Localization and Mapping (SLAM) algorithms, or Lidar Odometry and Mapping (LOAM) [16].

4 Initial Testing

Before moving to outdoor flying tests of the designed platform, the initial test is performed in an indoor environment, and it is limited to testing the LiDAR system (LiDAR, servo, microcomputer, battery, interface elements and connectors) when the drone is stationary. The width, length and height of the room are 4, 7 and 3 m, respectively. The generated point cloud is shown in Figure 6(a). Color distribution of the point cloud is based on elevation. The horizontal and vertical FoVs of the LiDAR system in this test are 270° and 360°, respectively. The LiDAR scans the environment in 2D lines, and each line contains 1,080 points. The number of lines of scanning in a sweep is dependent on the rotation speed of the servo. In this test, the rotation speed was set on 0.5 radians per second. Each sweep is π radians, so, one sweep was taken about 6.28 s to complete. The LiDAR scans 40 lines in a second, so, one sweep should contain about 251 lines and almost 270,000 points. The point cloud shown in Figure 6(a) is generated by 13 sweeps, and contains 3.2 million points. Each sweep has about 250,000 points. Some points are eliminated by the filtering node.

In order to check the accuracy of the collected point cloud, the same space was scanned with a higher accuracy 3D LiDAR scanner (FARO Focus3D) to generate a ground truth point cloud. FARO Focus3D is a 3D laser scanner with the accuracy of 2 mm, which can scan about one million points per second [26][22].

(a) Interfacing part for vertically mounting

(b) Platform with vertial LiDAR

(c) Interfacing part for inclined mounting

(d) Platform with inclined LiDAR
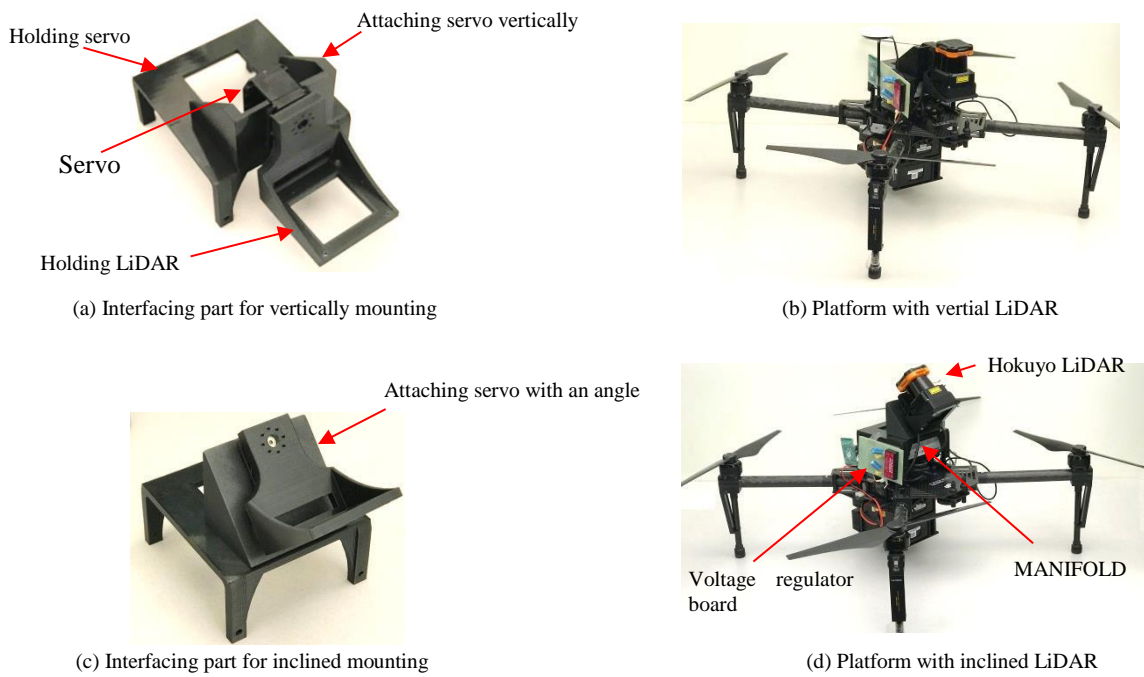
Figure 5. LiDAR-equipped UAV platform

(a) Generated point cloud by the designed platform

(b) Segment of point cloud

(c) Reference segment using FARO

(d) Comparison distance distribution histogram (m)

(e) Compared segment coloured based on distances from the reference segment
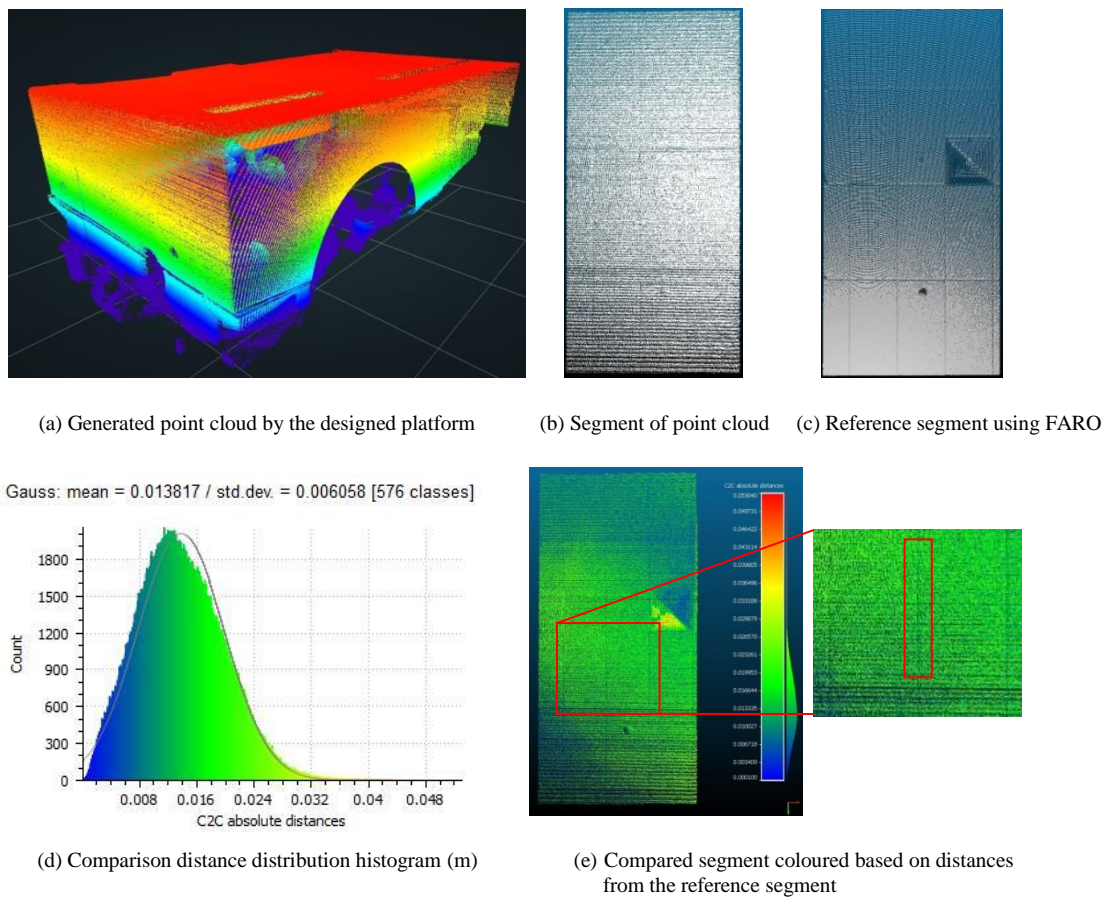
Figure 6. Initial testing results

A segment of the ceiling with the dimensions of 2.3 m × 4.7 m is selected (Figure 6(b)) and compared as cloud-to-cloud distance by CloudCompare software, where the distance of each point of the compared cloud is measured to its nearest neighbor in the reference cloud.

The two point clouds were aligned to each other manually in CloudCompare by picking five equivalent point pairs. Each segment contains about 250,000 points. The segment point cloud from FARO (Figure 6(c)) is considered as the reference cloud. The distance distribution histogram of the comparison is shown in Figure 6(d). Gaussian distribution is used in this computation, and the mean of the distribution is 1.4 cm with the standard deviation of 0.6 cm.

As shown in Figure 6(e), the gaps between the drop ceilings tiles of the room are visible. The width of these gaps is about 2 cm, which is greater than the calculated error. Assuming that these gaps are similar in size to some large cracks that could be detected on the actual structure during inspection, the accuracy of the point cloud collected by the platform can be considered enough to detect this size of cracks.

5   Conclusion and future work

In this study, a LiDAR-equipped UAV platform is designed to collect 3D point cloud data using a 2D LiDAR scanner. The design satisfies the main identified requirements and constraints for structural inspection. The platform is realized and tested in an indoor environment in a stationary mode.

Our future work includes: (1) applying the LOAM method integrated with an IMU to register the point cloud when the UAV is flying, and (2) testing the platform in the outdoor environment and defining the size of the defects that can be detected based on the accuracy of the data..

Acknowledgment

References

[1] Kim M., Sohn H. and Chang C. Localization and Quantification of Concrete Spalling Defects using Terrestrial Laser Scanning. *Journal of Computing in Civil Engineering,* 29 (6): 04014086, 2014.

[2] Liu W., Chen S. and Hauser E. LiDAR-based Bridge Structure Defect Detection. *Experimental Techniques,* 35 (6): 27-34, 2011.

[3] Adhikari R., Moselhi O. and Bagchi A. Image-Based Retrieval of Concrete Crack Properties for Bridge Inspection. *Automation in Construction,* 39180-194, 2014.

[4] Teza G., Galgaro A. and Moro F. Contactless Recognition of Concrete Surface Damage from Laser Scanning and Curvature Computation. *NDT & E International,* 42 (4): 240-249, 2009.

[5] Olsen M.J., Kuester F., Chang B.J. and Hutchinson T.C. Terrestrial Laser Scanning-Based Structural Damage Assessment. *Journal of Computing in Civil Engineering,* 24 (3): 264-272, 2009.

[6] Laefer D.F., Truong-Hong L., Carr H. and Singh M. Crack Detection Limits in Unit Based Masonry with Terrestrial Laser Scanning. *NDT & E International,* 62 (1): 66-76, 2014.

[7] Freimutha H., Müllera J. and Königa M. Simulating and executing UAV-assisted inspections on construction sites. In *34th International Symposium on Automation and Robotics in Construction and Mining,* pages 647-655, 2017.

[8] Yoder L. and Scherer S. Autonomous exploration for infrastructure modeling with a micro aerial vehicle. In *Field and Service Robotics,* pages 427-440, 2016.

[9] Bolourian N., Soltani M.M., Albahria A. and Hammad A. High level framework for bridge inspection using LiDAR-equipped UAV. In *Proceedings of the International Symposium on Automation and Robotics in Construction,* pages 1-6, Taipei, Taiwan, 2017.

[10] Zink J. and Lovelace B. Unmanned Aerial Vehicle Bridge Inspection Demonstration Project. 2015.

[11] Transport Canada. *, Canadian Aviation Regulations (CARs) and Standards.* 603.06, Sections 2017.

[12] Wallace L., Lucieer A., Watson C. and Turner D. Development of a UAV-LiDAR System with Application to Forest Inventory. *Remote Sensing,* 4 (6): 1519-1543, 2012.

[13] Guldur B. and Hajjar J.F. Laser-based condition assessment assistant for bridges. In *Proceedings of International Symposium Non-Destructive Testing in Civil Engineering,* , 2015.

[14] Bachrach A., Prentice S., He R. and Roy N. RANGE–Robust Autonomous Navigation in GPS-denied Environments. *Journal of Field Robotics,* 28 (5): 644-666, 2011.

[15] Honkavaara E., Kaivosoja J., Mäkynen J., Pellikka I., Pesonen L., Saari H., Salo H., Hakala T., Marklelin L. and Rosnell T. Hyperspectral Reflectance Signatures and Point Clouds for Precision Agriculture by Light Weight UAV Imaging System. *ISPRS Ann.Photogramm.Remote Sens.Spat.Inf.Sci,* 7353-358, 2012.

[16] Zhang J. and Singh S. LOAM: Lidar odometry and

mapping in real-time. In *Robotics: Science and System* , 2014.

[17] Winkvist S., Rushforth E. and Young K. Towards an Autonomous Indoor Aerial Inspection Vehicle. *Industrial Robot: An International Journal,* 40 (3): 196-207, 2013.

[18] Li Z., Yan Y., Jing Y. and Zhao S. The Design and Testing of a LiDAR Platform for a UAV for Heritage Mapping. *The International Archives of Photogrammetry, Remote Sensing and Spatial Information Sciences,* 40 (1): 17, 2015.

[19] DJI Co. Matrice 100. On-line: https://www.dji.com/matrice100/info,.

[20] HOKUYO AUTOMATIC CO. Distance data output UTM-30LX. On-line: https://www.hokuyo-aut.jp/search/single.php?serial=169,.

[21] DJI Co. Manifold. On-line: https://www.dji.com/manifold, Accessed: 2018.

[22] BOGOSIAN, B., GHARAKHANIAN, N., KHANOYAN, G., TOORIAN, A. and OHANIAN, R., 2016. *3D Scanning Assembly.* Glendale Community College.

[23] Bertussi S. Spin_hokuyo. On-line: http://wiki.ros.org/spin_hokuyo, Accessed: 27/07/2017.

[24] Coleman D. Rviz package summary. On-line: *http://*wiki.ros.org/rviz, Accessed: 15/6/2016.

[25] Sprickerhof J. Rosbag package summary. On-line: http://wiki.ros.org/rosbag, Accessed: 16/6/2015.

[26] Faro Inc., 2012. *Faro Laser Scanner Focus 3D X 130 -NEO-Tech.* Faro Inc.

[27] Venator E. PCL package summary. On-line: http://wiki.ros.org/pcl, Accessed: 20/05/2015.

[28] STORMBEE Co. Stormbee demo days. On-line: http://www.stormbee.eu/, Accessed: 2017.

[29] dhuber. Futuristic infrastructure inspection in pennsylvania. On-line: http://aria.ri.cmu.edu/archives/category/media, Accessed: 11/04/2014.